Voyager 1 Observes Low-Energy Galactic Cosmic Rays in a Region Depleted of Heliospheric Ions

E. C. Stone *et al.*

Science **341**, 150 (2013);
DOI: 10.1126/science.1236408

but there is a statistically significant difference from the spiral field direction in the HDR, namely $\lambda_A - \lambda_P = 17° \pm 1°$ and $\delta_A - \delta_P = 14° \pm 2°$ as shown in Fig. 2. The magnetic polarity of the magnetic field in the HDR indicates that it has moved from the southern hemisphere to the position of V1 in the northern hemisphere. The small departure from the spiral field direction might be the result of a flow that carried the magnetic field northward in the heliosheath to the location of V1. It has been suggested that such a flow moves northward in the heliosheath between a "magnetic wall" or "magnetic barrier" and the heliopause at the latitude of V1 (*5*, *25*).

Increasingly strong magnetic fields from the middle of 2010 until at least the middle of 2011 (possibly extending up to 150, 2012 as shown in this paper) were reported in (*26*), where it was suggested that these strong magnetic fields might be related to a magnetic wall or magnetic barrier. Thus, it is conceivable that the HDR corresponds to this northward heliosheath flow near the heliopause, and the boundary of the HDR represents a boundary of material that was moving radially closer to the Sun. The strong magnetic fields observed from mid-2010 to 270, 2012 could be an interaction region that extends into the HDR, produced by the collision of these two flows. The stronger magnetic field in the HDR might be produced in response to the reduction of pressure owing to the absence of energetic particles. The absence of energetic particles could indicate that magnetic lines passing V1 were no longer connected to their source (the blunt termination shock), because V1 crossed a topologic boundary in the magnetic field of the inner heliosheath beyond the last magnetic connection point to the termination shock (*27*). Alternatively, the energetic particles could have escaped into interstellar space, if the heliosheath magnetic field reconnected with the interstellar magnetic field beyond the position of V1.

References and Notes

1. E. C. Stone *et al.*, *Science* **309**, 2017–2020 (2005).
2. L. F. Burlaga *et al.*, *Science* **309**, 2027–2029 (2005).
3. R. B. Decker *et al.*, *Science* **309**, 2020–2024 (2005).
4. N. V. Pogorelov *et al.*, *Astrophys. J. Lett.* **750**, L4 (2012).
5. H. Washimi *et al.*, *Mon. Not. R. Astron. Soc.* **416**, 1475–1485 (2011).
6. M. Opher *et al.*, *Astrophys. J.* **734**, 71 (2011).
7. S. M. Krimigis, E. C. Roelof, R. B. Decker, M. E. Hill, *Nature* **474**, 359–361 (2011).
8. E. C. Stone *et al.*, *Proc. 32nd Int. Cosmic Ray Conf.* **12**, 29 (2011).
9. R. B. Decker, S. M. Krimigis, E. C. Roelof, M. E. Hill, *Nature* **489**, 124–127 (2012).
10. E. C. Stone *et al.*, *Science* **341**, 150–153 (2013).
11. W. R. Webber, F. B. McDonald, *Geophys. Res. Lett.* **40**, 1665–1668 (2013).
12. K. Behannon *et al.*, *Space Sci. Rev.* **21**, 235 (1997).
13. D. B. Berdichevsky, Voyager mission, detailed processing of weak magnetic fields; constraints to the uncertainties of the calibrated magnetic field signal in the Voyager missions (2009); http://vgrmag.gsfc.nasa.gov/Berdichevsky-VOY_sensor_opu090518.pdf.
14. E. C. Stone *et al.*, *Space Sci. Rev.* **21**, 355 (1977).
15. L. F. Burlaga, N. F. Ness, *J. Geophys. Res.* **116**, A05102 (2011).
16. V. Florinski, G. P. Zank, N. V. Pogorelov, *J. Geophys. Res.* **110**, A07104 (2005).
17. S. N. Borovikov, N. V. Pogorelov, G. P. Zank, I. A. Kryukov, *Astrophys. J.* **682**, 1404–1415 (2008).
18. E. N. Parker, *Interplanetary Dynamical Processes* (Interscience Publishers, New York, 1963).
19. M. Opher *et al.*, *Nature* **462**, 1036–1038 (2009).
20. N. V. Pogorelov, J. Heerikhuisen, J. J. Mitchell, I. H. Cairns, G. P. Zank, *Astrophys. J.* **695**, L31–L34 (2009).
21. V. Izmodenov *et al.*, *Space Sci. Rev.* **146**, 329–351 (2009).
22. J. Heerikhuisen *et al.*, *Astrophys. J. Lett.* **708**, L126–L130 (2010).
23. P. C. Frisch, *Proc. 10th Ann. Int. Astrophys. Conf. AIP Conf. Proc.* **1436**, 239 (2012).
24. G. P. Zank *et al.*, *Astrophys. J.* **763**, 20 (2013).
25. H. Washimi, T. Tanaka, *Space Sci. Rev.* **78**, 85–94 (1996).
26. L. F. Burlaga, N. F. Ness, *Astrophys. J.* **749**, 13 (2012).
27. D. J. McComas, N. A. Schwadron, *Astrophys. J.* **758**, 19 (2012).
28. www.srl.caltech.edu/ACE/ASC/coordinate_systems.html

Acknowledgments: T. McClanahan and S. Kramer provided support in the processing of the data and D. Berdichevsky computed correction tables for the three sensors on each of the two magnetometers. N.F.N. was partially supported by NASA grant NNX12AC63G to the Catholic University of America. L.F.B. was supported by NASA contract NNG11PN48P. The data are available at NASA's Virtual Heliospheric Observatory (http://vho.nasa.gov/), maintained within the Heliospheric Physics Laboratory at NASA's Goddard Space Flight Center.

Supplementary Materials

www.sciencemag.org/cgi/content/full/science.1235451/DC1
Supplementary Text
Fig. S1

21 January 2013; accepted 30 May 2013
Published online 27 June 2013;
10.1126/science.1235451

Voyager 1 Observes Low-Energy Galactic Cosmic Rays in a Region Depleted of Heliospheric Ions

E. C. Stone,[1]* A. C. Cummings,[1] F. B. McDonald,[2]† B. C. Heikkila,[3] N. Lal,[3] W. R. Webber[4]

On 25 August 2012, Voyager 1 was at 122 astronomical units when the steady intensity of low-energy ions it had observed for the previous 6 years suddenly dropped for a third time and soon completely disappeared as the ions streamed away into interstellar space. Although the magnetic field observations indicate that Voyager 1 remained inside the heliosphere, the intensity of cosmic ray nuclei from outside the heliosphere abruptly increased. We report the spectra of galactic cosmic rays down to ~3×10^6 electron volts per nucleon, revealing H and He energy spectra with broad peaks from 10×10^6 to 40×10^6 electron volts per nucleon and an increasing galactic cosmic-ray electron intensity down to ~10×10^6 electron volts.

A key objective of the Voyager Cosmic Ray Subsystem (*1*) is the determination of the intensity of galactic cosmic-ray (GCR) nuclei and electrons in the interstellar medium outside of the heliosphere. On 25 August 2012, Voyager 1 (V1) entered a region where the heliospheric ions were depleted and replaced by low-energy GCR nuclei and electrons. This would have been expected had V1 crossed the heliopause, the boundary separating the solar wind plasma and magnetic field from the interstellar plasma and magnetic field. However, there was no change in the direction of the magnetic field even though the field intensity abruptly increased by 60%, indicating that the magnetic field lines in this region originated at the Sun, not from interstellar space (*2*). So, V1 appears to have entered a previously unknown region that is depleted of energetic heliospheric ions and accessible to low-energy cosmic rays [see also (*3*, *4*)].

The first indication of a heliospheric depletion region was observed on 28 July 2012, when the intensity of protons from inside the heliosphere with energies 0.5 MeV $\leq E \leq$ 60 MeV abruptly decreased and subsequently recovered 5 days later (counting rates C and D in Fig. 1). A second decrease on 13 August lasted 8 days and was followed 4 days later by the durable entry of V1 into the heliospheric depletion region on 25 August. The magnetic field increased simultaneously with the decreases in energetic protons, suggesting that lower-energy plasma may also have escaped, with the resulting decrease in plasma pressure leading to a compression of the magnetic field (*2*).

The intensity changes for four distinct populations of energetic particles are strongly correlated as shown in Fig. 1. Because of their small mass, the GCR electrons have the smallest radii of gyration around the magnetic field lines, typically 0.0006 astronomical units (AU) for a

[1]California Institute of Technology, Pasadena, CA 91125, USA. [2]University of Maryland, College Park, MD 20742, USA. [3]NASA/Goddard Space Flight Center, Greenbelt, MD 20771, USA. [4]New Mexico State University, Las Cruces, NM 88003, USA.

*Corresponding author. E-mail: ecs@srl.caltech.edu
†Deceased

10-MeV electron in a heliosheath magnetic field of 0.4 nT. Because V1 crosses that distance in <1.5 hours, the electrons provide the sharpest indication of when V1 crossed the boundary of the region where there is enhanced access of GCRs from outside. The edges of the regions of enhanced electron intensities are closely aligned with the five boundaries of the regions of enhanced magnetic field that occurred on day of the year (DOY) 210.6, 215.6, 225.7, 233.5, and 237.7 (*2*). The heavier ions have larger gyroradii that result in broader intensity transitions, as seen in the counting rate of >70-MeV cosmic-ray nuclei. For example, V1 crosses the 0.025-AU gyroradius of a 100-MeV proton in ~2.5 days. Anomalous cosmic rays (ACRs) are also accelerated in the outer heliosphere, and at energies below ~100 MeV per nucleon their intensity

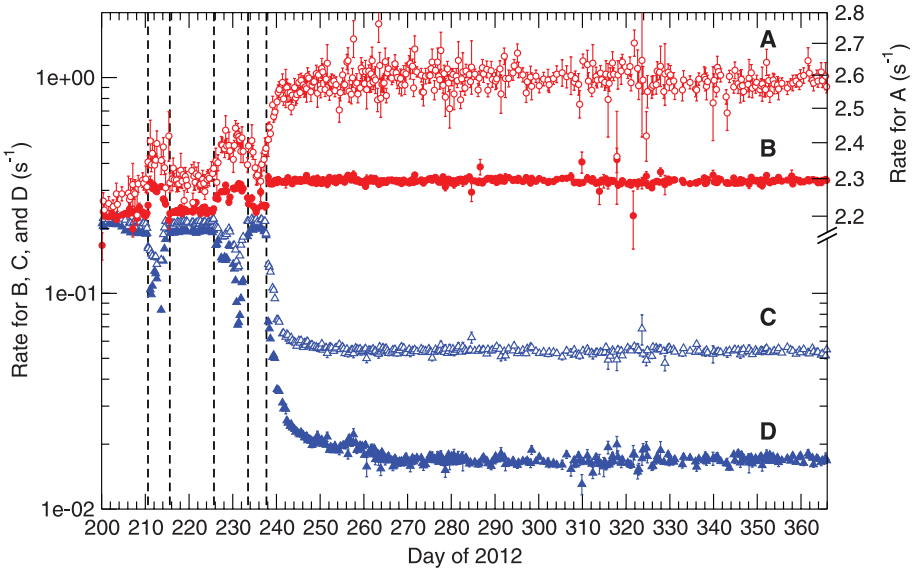

Fig. 1. The counting rates (6-hour averages) of four different energetic particle species in the vicinity of the depletion region. (**A**) (*y* axis on right) GCR nuclei (mainly protons with $E > 70$ MeV) penetrating the High Energy Telescope 1 (HET 1). (**B**) (*y* axis on left) GCR electrons with energies between 6 and ~100 MeV observed by the Electron Telescope (TET). (**C**) (*y* axis on left) Protons with 7 to 60 MeV stopping in HET 1 (rate shown is divided by 11.55) are mainly anomalous cosmic rays before 2012/238 (25 August) and galactic cosmic rays after that. (**D**) (*y* axis on left) Low-energy particles observed in the LET A (rate shown is divided by 124.5) are mainly protons with 0.5 to ~30 MeV accelerated at the termination shock and in the heliosheath plus a scaled background rate of 0.017 s^{-1} because of higher-energy nuclei. Three distinct periods in 2012 on days 210 to 215 (28 July to 2 August), 226 to 233 (13 to 20 August), and from 238 (25 August) are indicated by vertical lines corresponding to the magnetic boundaries of the depletion region (*2*). The simultaneous intensity changes coincide with abrupt increases and decreases in the magnitude of the magnetic field, suggesting that, after two brief encounters with a depletion region or regions, V1 durably entered a broad depletion region on 25 August (DOY 238).

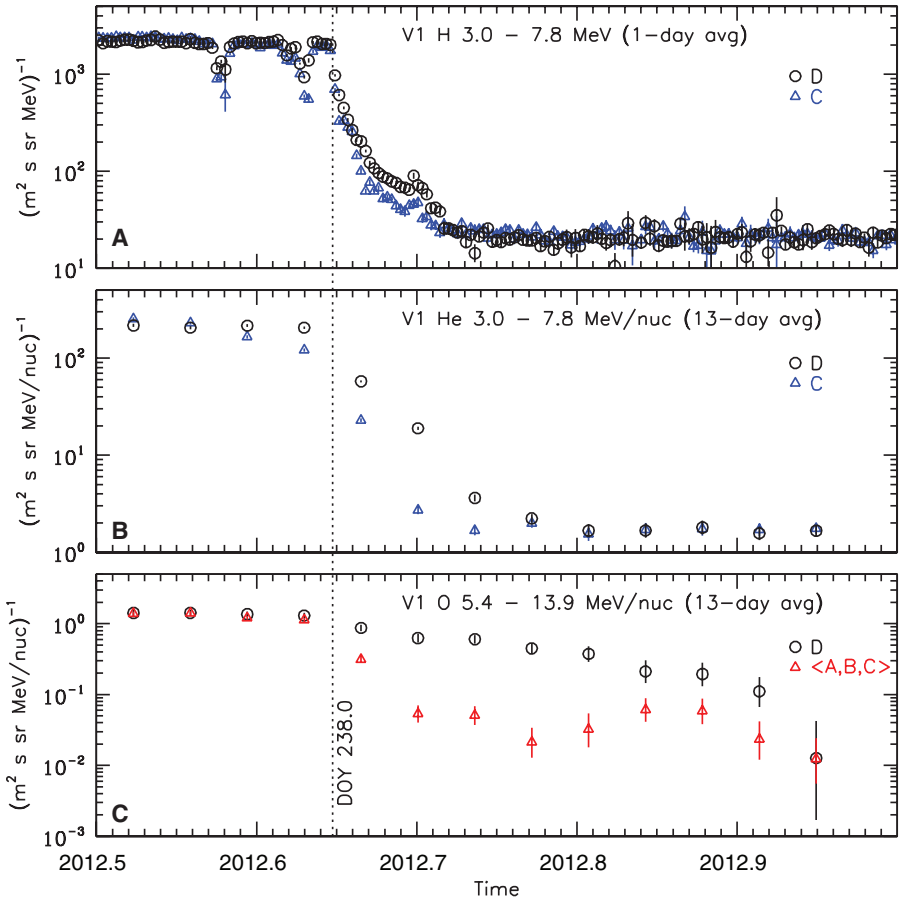

Fig. 2. Intensities of H, He, and O from V1 for the last half of 2012. (**A**) One-day average intensities of H with 3.0 to 7.8 MeV. Intensities are shown for two of the four LETs [see (*1*) for arrangement of the telescopes]. The bore sight of LET D is pointed roughly perpendicular to the magnetic field direction. The bore sight of LET C is oriented at 90° to that of LET D. (**B**) Similar to (A) except for 13-day averages of the intensities of He with 3.0 to 7.8 MeV per nucleon. (**C**) Similar to (B) except for O with 5.4 to 13.9 MeV per nucleon, and the average intensity from the LET A, B, and C is plotted instead of only LET C, in order to improve the statistical significance of the result. The LET A bore sight is oppositely directed to that of LET C, and the bore sights of LET A, B, and D form an orthogonal set. Error bars indicate statistical uncertainties (±1 σ).

greatly exceeds that of GCRs. As seen by the intensity of 7- to 60-MeV protons in Fig. 1, the intensities of ACRs also decrease in the depletion regions as they escape out of the heliosphere. Their disappearance beginning on DOY 238 reveals the intensity of GCRs of the same energy that have flowed into the depletion region from outside.

Voyager has four Low-Energy Telescopes (LETs) arranged in an orthogonal array (*1*). As illustrated in Fig. 2, there are substantial differences in intensity among the telescopes over extended periods. LET D is oriented so that it observes protons with pitch angles from 50 to 100 to the spiral magnetic field, which is pointing outward along the spiral direction (*2*), so LET D is sensitive to ions moving outward along the field ($\theta < 90°$) and also inward ($\theta > 90°$). LET C observes protons with pitch angles of from 110 to 160, so it is sensitive to ions coming inward along the spiral field.

These ions originate at the termination shock or in the heliosheath and diffuse mainly along the spiral magnetic field. Before 28 July, there was sufficient scattering on the field line that the intensity of ions in LET C was the same as in LET D. However, during the first two decreases, the intensity of ions diffusing inward toward LET C was significantly lower than in LET D, indicating some of the ions spiraling outward were lost and not scattered back toward V1.

After the boundary crossing on 25 August (DOY 238), the intensity of H ions (protons) in LET C dropped much more rapidly than the intensity of protons in LET D. The two rates converged after 2012.72 (DOY 263), indicating that low-energy protons from the heliosphere were no longer dominating the intensity near 5 MeV at V1. Instead, the intensity was isotropic, as expected if the remaining protons are low-energy GCRs diffusing in along the magnetic field.

Figure 2 also shows similar anisotropies for He and O. Although longer time averages are required because of the lower intensities, there is evidence for losses in LET C during the events before DOY 238 and for extended periods after. At those times, the outward flow was observed in LET D, while LET C was already observing a lower intensity of isotropic GCRs diffusing inward along the magnetic field. The longer persistence of the heavier heliospheric ions is consistent with the expectation that singly ionized 5–MeV per nucleon He^+ and 9–MeV per nucleon O^+ with gyroradii of 0.022 and 0.12 AU, respectively, will have larger scattering mean free paths and will be scattered into the loss cone more slowly than 5-MeV H^+, which has a gyroradius of 0.0054 AU.

The disappearance of most of the heliospheric ions after 25 August 2012 provides an opportunity to examine the energy spectra of GCRs to lower energies than previously possible (*4*). Figure 2 shows that GCR H and He dominate the 3– to 7.8–MeV per nucleon energy range

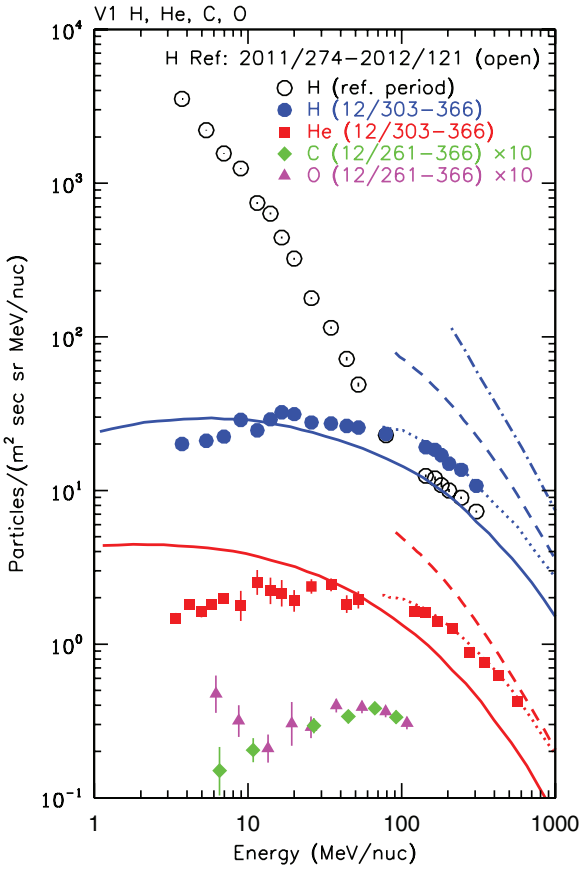

Fig. 3. Differential energy spectra of H, He, C, and O from V1. Two spectra are shown for H: one for a reference period before the depletion region was reached, 2011/274 to 2012/121, and one for a new period within the depletion region, 2012/303 to 366. For these two H spectra, intensities from all four LETs were averaged together. At higher energies, >57 MeV, only intensities from HET 2 are shown. The same telescopes were used in deriving the He spectrum for the period 2012/303 to 366. For C, intensities from all four LETs were used, and at higher energies, >20 MeV per nucleon, intensities from both HETs were averaged together. For O with 5.4 to 17.1 MeV per nucleon, only LET A, B, and C were used in order to minimize the contribution from heliospheric particles. For O with 17.1 to 21.6 MeV per nucleon, only HET 2 was used, and for energies >21.6 MeV per nucleon, intensities from both HETs were averaged together. The C and O spectra are for the period 2012/261 to 366. Several estimates of the local interstellar galactic cosmic ray H and He spectra are shown. The solid lines are model a from Ip and Axford (*13*). The dotted lines represent the leaky-box model from Webber and Higbie (*14*). The dashed lines are the DC model from Moskalenko *et al.* (*19*), and the dot-dash line for H is from Fisk and Gloeckler (*20*). Error bars indicate statistical uncertainties (±1 σ).

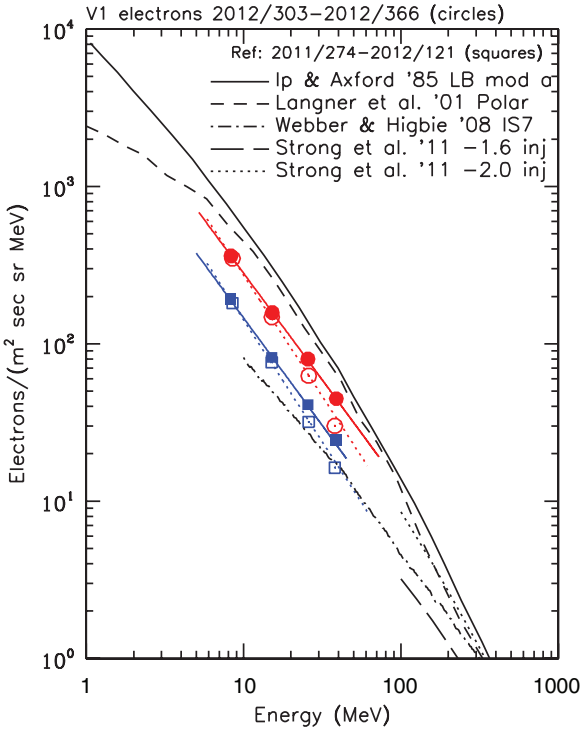

Fig. 4. Differential energy spectra of electrons from the V1 TET. Two pairs of spectra are shown, one pair for a reference period before the new region was reached, 2011/274 to 2012/121, and one pair for a period within the new region, 2012/303 to 366. The open symbols represent spectra derived by using response functions from a prelaunch accelerator calibration. The solid symbols use response functions from a GEANT4 simulation. The intensity differences in the solid and open symbols for a given period are an indication of the systematic uncertainly in the electron spectrum that is proportional to $E^{-1.45 \pm 0.09}$ in the new region. The method used in deriving the energy spectra is described in the supplementary materials. Three estimates of the local interstellar GCR electron spectrum are shown. The solid line is model a from Ip and Axford (*13*), the dot-dash line represents model IS7 from Webber and Higbie (*21*), the short-dashed line represents the polar model from Langner *et al.* (*16*), and the long-dashed and dotted lines are from Strong *et al.* (*17*) for electron source spectra proportional to $E^{-1.6}$ and $E^{-2.0}$, respectively, and include positrons.

from ~2012.77 (DOY 282) onward, because the intensity apparently became isotropic at that time, consistent with the expectation for GCRs. Figure 3 shows the energy spectra for the period 2012/303 to 366 for H and He from 3 to several hundred MeV per nucleon along with an energy spectrum of H from a period before the onset of the recent activity. This reference spectrum shows the dominance of the spectrum by the termination shock particle and ACR heliospheric particle populations below ~100 MeV per nucleon during this time. These particles have largely streamed away in the more recent period (DOY 303 to 366), replaced by the inflow of low-energy GCRs.

However, it is uncertain whether GCRs have fully unimpeded access into this region. In addition, the GCR intensity immediately outside the heliosphere may be lower than the galactic intensity because of modulation in the local interstellar medium (*5*–*7*). Recent models indicate a reduction of ~25 to ~40% in the intensity of 100-MeV protons, with corresponding positive radial gradients of ~0.5 and ~0.9%/AU near the heliopause (*7*), although other models suggest that there should be no interstellar gradient (*8*). The time dependence of the observed intensities after the disappearance of heliospheric protons (DOY 270 to 366 in Fig. 1) corresponds to gradients of –1.4 ± 0.9%/AU for 7- to 60-MeV protons and –1.0 ± 0.4%/AU for >70-MeV GCR nuclei, mainly protons. The gradient of 6- to 100-MeV electrons is also small, only −0.6 ± 0.6%/AU from DOY 239 to 366. Thus, there is no evidence for a positive radial gradient in the current region.

The GCR H and He spectra have the same shape from ~3 to 346 MeV per nucleon. The H/He ratio has been determined in three energy ranges corresponding to different telescope and/or operation modes of the instrument. In the lowest energy band, 3 to 7.8 MeV per nucleon, we find the H/He ratio to be 11.9 ± 0.4. In the 7.8–to–57 MeV per nucleon band, the ratio is 12.9 ± 0.6, and in the highest energy interval, 134 to 346 MeV per nucleon, the ratio is 12.6 ± 0.3. These uncertainties are purely statistical, and there may be systematic uncertainties as well. However, the reasonably good agreement of the ratios across the range from 3 to 346 MeV per nucleon suggests that systematic uncertainties are likely small. The peak intensities of the GCR spectra of H and He are in the ~10– to 40–MeV per nucleon energy range.

The H/He ratio of 12.9 ± 0.6 in the energy region of the peak in the spectra is consistent with the recommended abundance in the solar photosphere, 12.6 (*9*). It differs from previous cosmic-ray observations of 4.7 ± 0.5 at 100 MeV per nucleon observed at 1 AU, where the spectra and abundance ratios are modified by the effects of solar modulation (*10*). It also differs from the ACR ratio of 4.1 (*11*), indicating that ACRs do not dominate GCRs outside the heliosphere as has been suggested (*12*).

The leaky-box model of Ip and Axford (*13*) addresses the low-energy portion of the GCR spectra (Fig. 3). Their model appears to have about the right peak intensity for H, but the energy of the peak is lower than observed. For He, both the peak intensity and the energy of the peak are somewhat displaced from the observations. At higher energies, >70 MeV per nucleon, the leaky-box model spectra from Webber and Higbie (*14*) are in good agreement with the observed H and He spectra.

Also shown in Fig. 3 are C and O spectra for 2012/261 to 366. This longer period improves the statistical significance of the observations and is justified by the intensity-versus-time profile of O with 5.4 to 13.9 MeV per nucleon for LETs A, B, and C shown in Fig. 2. In constructing the energy spectra for O in Fig. 3, the LET D telescope was not used, because it has a more persistent heliospheric contribution resulting from its bore sight looking nearly perpendicular to the magnetic field direction. Even ignoring LET D, there may be some residual heliospheric contribution present below ~10 MeV per nucleon. The C and O energy spectra above ~10 MeV per nucleon are very similar, with the peak C intensity occurring at ~70 MeV per nucleon. The C/O ratio for the energy range 21.6 to 106 MeV per nucleon is 0.95 ± 0.06, consistent with GCR observations at higher energies at 1 AU (*10*, *15*) and not with the ACR ratio of 0.005 (*11*). All previous measurements below ~100 MeV per nucleon represent particles decelerated from much higher energies by the solar modulation process.

The intensity of electrons with ~6 to 100 MeV had jumps in concert with the GCR nuclei (Fig. 1), indicating that V1 is observing GCR electrons in this energy range as opposed to electrons accelerated in the heliosphere. The ratio of intensities of the two periods shown in Fig. 4 is roughly a factor of two over the energy range shown, indicating an energy-independent diffusive mean free path for 6- to 60-MeV electrons.

The energy spectrum for the new region is proportional to $E^{-1.45 \pm 0.09}$ and has a spectral shape that is very similar to the theoretical estimates of the interstellar electron spectrum of Ip and Axford (*13*) and Langner *et al.* (*16*), but the overall intensity is about a factor of two below those estimates. The observed intensity exceeds an extrapolation of the spectrum from a diffusion model by Strong *et al.* (*17*) that assumes an electron source spectrum proportional to $E^{-1.6}$ below a few GeV, as implied by fits to radio synchrotron emission. A source spectrum of E^{-2} would better match the electron spectrum (Fig. 4) but would not be consistent with the radio observations without other adjustments to the model.

The presence of a region having a spiral magnetic field, but depleted of energetic heliospheric particles and accessible by low-energy GCR nuclei and electrons, is an important feature of the interaction between the heliosphere and the local interstellar medium. It has been suggested that this could be a disconnection region where the spiral field has been convected far enough beyond the termination shock so that there is not an effective connection to the source of anomalous cosmic rays at the termination shock (*18*). Further development of this and other possible models will benefit our understanding of the region beyond 122 AU that Voyager 1 is now exploring.

References and Notes

1. E. C. Stone *et al.*, *Space Sci. Rev.* **21**, 355 (1977).
2. L. F. Burlaga, N. F. Ness, E. C. Stone, *Science* **341**, 147–150 (2013); 10.1126/science.1235451.
3. S. M. Krimigis *et al.*, *Science* **341**, 144–147 (2013); 10.1126/science.1235721.
4. W. R. Webber, F. B. McDonald, *Geophys. Res. Lett.* **40**, 1665–1668 (2013).
5. K. Herbst, B. Heber, A. Kopp, O. Sternal, F. Steinhilber, *Astrophys. J.* **761**, 17 (2012).
6. K. Scherer *et al.*, *Astrophys. J.* **735**, 128 (2011).
7. R. D. Strauss, M. S. Potgieter, S. E. S. Ferreira, H. Fichtner, K. Scherer, *Astrophys. J.* **765**, L18 (2013).
8. J. R. Jokipii, in *The Outer Heliosphere: The Next Frontiers*, K.Scherer, H. Fichtner, H. J. Fahr, E. Marsch, Eds. (Pergamon, New York, 2001), pp. 513–519.
9. K. Lodders, *Astrophys. J.* **591**, 1220–1247 (2003).
10. J. A. Simpson, *Annu. Rev. Nucl. Part. Sci.* **33**, 323–382 (1983).
11. A. C. Cummings, E. C. Stone, C. D. Steenberg, *Astrophys. J.* **578**, 194–210 (2002).
12. K. Scherer, H. Fichtner, S. E. S. Ferreira, I. Büsching, M. S. Potgieter, *Astrophys. J.* **680**, L105–L108 (2008).
13. W.-H. Ip, W. I. Axford, *Astron. Astrophys.* **149**, 7 (1985).
14. W. R. Webber, P. R. Higbie, *J. Geophys. Res.* **114**, A02103 (2009).
15. J. S. George *et al.*, *Astrophys. J.* **698**, 1666–1681 (2009).
16. U. W. Langner, O. C. de Jager, M. S. Potgieter, in *Proceedings of the 27th International Cosmic Ray Conference*, 7 to 15 August 2001, Hamburg, Germany (International Union of Pure and Applied Physics, Berlin, 2001), vol. 10, pp. 3992–3995.
17. A. W. Strong, E. Orlando, T. R. Jaffe, *Astron. Astrophys.* **534**, A54 (2011).
18. D. J. McComas, N. A. Schwadron, *Astrophys. J.* **758**, 19 (2012).
19. I. V. Moskalenko, A. W. Strong, J. F. Ormes, M. S. Potgieter, *Astrophys. J.* **565**, 280–296 (2002).
20. L. A. Fisk, G. Gloeckler, *Astrophys. J.* **744**, 127 (2012).
21. W. R. Webber, P. R. Higbie, *J. Geophys. Res.* **113**, A11106 (2008).

Acknowledgments: This work was supported by NASA (NNN12A012). This paper is dedicated to the memory of Frank McDonald, whose leadership in the cosmic-ray investigation on Voyager began in 1972. His contributions continued until the day of his passing, just after Voyager 1 durably entered the depletion region and fulfilled his vision of observing low-energy galactic cosmic rays from the local interstellar medium. This paper benefited substantially from discussions during meetings of the International Team on the Physics of the Heliopause at the International Space Science Institute in Bern, Switzerland.

Supplementary Materials

www.sciencemag.org/cgi/content/full/science.1236408/DC1
Supplementary Text
Fig. S1
References

11 February 2013; accepted 24 May 2013
Published online 27 June 2013;
10.1126/science.1236408